



The role of gas bubbles and liquid slug lengths on mass transport in the Taylor flow through capillaries

Gorazd Berčič* and Albin Pintar

Laboratory for Catalysis and Chemical Reaction Engineering, National Institute of Chemistry, Hajdrihova 19, P.O. Box 3430, SI-1001 Ljubljana, Slovenia

(Accepted 1 July 1997)

Abstract—Gas-liquid and liquid-solid mass transfers were studied in capillaries under Taylor flow regime. The influence of the capillary diameter, unit cell length and gas hold-up on measured $k_L a$ and $k_S a$ coefficients was correlated by simple correlation, which showed that in both cases the mass transport is mostly determined by the liquid slug length and velocity. The results demonstrated that the contribution of the mass transferred in the thin liquid film surrounding the gas bubble is not dominant. The conclusions agreed with the predictions made on the basis of a model developed by means of RTD measurements which were carried out in the same capillaries. The results obtained during catalytic hydrogenation of nitrite ions can also be explained in view of new findings. © 1997 Elsevier Science Ltd

Keywords: Monolith reactor; Taylor flow; mass transfer; residence time distribution; modelling; catalytic liquid-phase nitrite hydrogenation.

INTRODUCTION

Although monolith catalytic blocks were designed first of all for converting exhaust gases from the Otto engines, they have become attractive also in the field of three-phase catalytic reactions. Cybulski *et al.* (1993) showed that monolith reactors are a viable alternative to the conventional three-phase reactors such as trickle bed and slurry reactors. The most important work concerning the study of mass transport in capillaries was done by the group of Andersson, who studied fundamentals of the liquid-solid mass transfer (Hatzilantonidou and Andersson, 1982) and gas-liquid mass transfer (Irandoost *et al.*, 1992). The correlations which they derived for the prediction of mass transfer coefficients were used in most of the works dealing with modelling of systems where two-phase reactions take place in monolith reactors (Cybulski *et al.*, 1993; Irandoost and Andersson, 1988; Wärnå *et al.*, 1994). Since for the mass transfer in the Taylor flow regime, the thickness of the liquid film surrounding the gas bubble and the recirculation within the liquid slug are of the highest importance, many studies were concerned with the characterisation of particular contributions. Among the first to study the film thickness in the segmented

flow of gas and liquid through capillaries experimentally were Fairbrother and Stubbs (1935), Taylor (1960) and Marchessault and Mason (1960). The first theoretical studies based on lubrication theory were done by Bretherton (1961). His results are in close agreement with recent studies made on the basis of finite element analysis by Shen and Udell (1985) and Edvinsson and Irandoost (1996). The results allow to predict the film thickness as well as the flow pattern within the liquid slug. However, the qualitative correlation between flow patterns and the mass transfer is not discussed. Pedersen and Horváth (1981) studied the axial dispersion in the reactor with segmented flow and developed a simple lumped parameter model on the basis of RTD measurements using tracer inputs.

Recently, Patrick *et al.* (1995) studied RTD in a three-phase monolith reactor. They found out that the liquid is substantially well mixed and that the RTD curve from the monolith section of their apparatus can be well approximated by a series of 1.15 perfectly mixed vessels. However, they provide no data about the average lengths of gas bubbles and liquid slugs formed in the monolith channels, but correlate the total residence time as a function of liquid and/or gas flow rate. A large scattering of experimentally determined values showed that in this particular case operation at that scale was not stable. From the results of RTD measurements one can also assume that the distribution of liquid and gas flow

*Corresponding author. Tel.: (+386-61) 1760282; fax: (+386-61) 1259244; email: gorazd.bercic@ki.si.

among channels in a monolith block is non-homogeneous, since the overall response is similar to the one obtained in a CSTR reactor.

While studies concerning determination of the film thickness and mass transfer between gas and liquid, as well as between liquid and solid, have been conducted in single channel-capillary reactors, all the measurements performed under reaction conditions have so far been made using multichannel commercial monolith blocks. Therefore, the conclusions drawn from single-channel experiments are not straightforward, mostly due to the non-uniform distribution of gas and liquid among channels in the monolith block. Since good distribution of phases is a critical factor for the monolith scale-up, special care should be paid to the design of gas-liquid distributors. Such distribution has usually been obtained using perforated plates (Irlandoust *et al.*, 1989), frittes (Crynes *et al.*, 1995), a rotary distributor (Wärnå *et al.*, 1994) or special needle distributors (Kawakami *et al.*, 1989).

Although authors agree that good gas-liquid distribution is important for the operation of monolith reactors, no one has tried to make all experiments, i.e. measurements of k_La , k_Sa , RTD and chemical reaction, in the same apparatus in order to obtain a common background for the comparison and characterisation of the most important factors in the segmented flow of liquid and gas through capillaries. The main objective of this study is to qualitatively and quantitatively present the influence of the most important parameters, such as velocity, unit cell length (UCL) and gas hold-up on the measured mass transfer coefficients and/or conversion of a model reactant. The axial dispersion was studied by RTD measurements and a simple model was developed and used in order to assess where the major part of the gas is transferred into the liquid and where the majority of reactants are converted.

EXPERIMENTAL

The k_La coefficients were determined by measuring the amount of methane dissolved in the water flowing upward through a single-glass capillary. The experiments were performed using 1.12 m long capillaries of different inside diameters (1.5, 2.5 and 3.1 mm) at 298 K and at ambient pressure. The capillaries were installed in a glass tube and shell heat exchanger, which was thermostated by the Haake DC3/K20 thermostat. Methane and water were fed to the PP tee connector from the opposite sides by means of two computer-controlled Masterflex peristaltic pumps. By means of silicon tubing, the test capillaries were closely connected to the remaining free port of the tee connector; the latter was shortened in order to reduce the dead volume. The stream of gas and liquid slugs leaving the capillary was led into the phase separator, where both phases were separated. The gas separator was tightly closed in order to prevent degassing of the liquid phase. The liquid was leaving the phase separator continuously through the siphon, while the gas

phase was discharged through 1 m long PE tube (ID 4 mm) to prevent the air to enter the separator. Five millilitres of liquid samples were taken from the siphon by a syringe and injected into the purgable organic carbon (POC) sparger of the Rosemount/Dohrmann DC-190 TOC analyser for methane determination.

The k_Sa coefficients were determined on the same experimental set-up by measuring the dissolution of benzoic acid into water. The preparation of the tube containing the benzoic channel was similar to that described in the paper of Hatzlantoniou and Andersson (1982). The concentration of dissolved benzoic acid in water was determined by use of a differential refractory index detector (Knauer) and a TOC analyser. The length of coated tubes ranged from 25 to 35 cm and the ID was 2.5 mm.

The RTD measurements were performed in the same experimental arrangement as for the determination of k_La coefficients. The inlet tee connector was closely coupled with a two-way micro solenoid valve (Takasago, model EXAKN-3), which was used for introducing the step input of tracer by switching between two water solutions with different concentrations of KMnO_4 , i.e. 20 and 60 mg/l, respectively. The tracer concentration was measured at two different locations (15.5 or 102 cm from the tee connector) using a UV-VIS spectrophotometer (Perkin Elmer, model Lambda 40) equipped with fibre optics cables and an extension cell which was mounted over the glass tube. Glycerine was used to match the refractory index of the glass tube to avoid refraction of the light at the outer wall of the tube. The concentration of KMnO_4 was measured continuously and the measured signal was recorded by computer. By means of calibration curves, which were measured by using solutions of known KMnO_4 concentrations, the concentration of KMnO_4 in liquid slugs was calculated. It should be noted that the signal varies almost linearly in the examined concentration range. The concentration measurements were carried out at a wavelength of 525 nm; typical scan rates were in the range from 10 to 20 samples per second, depending on the flow rate and the length of gas bubbles and liquid slugs.

To perform a model reaction in the same range of experimental conditions as they were used to determine the mass transfer coefficients a reaction between hydrogen and nitrite ions was carried out. For that purpose, the inside wall of ceramic capillaries was impregnated with an appropriate Pd catalyst. The length and ID of the catalytically active channel were 112 cm and 1.85 mm, respectively. The concentration of nitrite ions were up to 22 mg/L and were measured by means of a PE-FIAS module connected to the Lambda 40 UV-VIS spectrophotometer, using the standardised naphthylamine method. Pure hydrogen (99.9%) was employed as a reducing agent. No attempt was made to measure reaction kinetics in detail. The investigated reaction served only as a tool to resolve whether the reaction takes place in the liquid film or in the liquid slug.

Analysis of experimental data

During the experiments the gas and liquid slug lengths were controlled and adjusted by changing the time interval for dosing gas or liquid by two independently driven peristaltic pumps. It was possible to increase the cell-velocity simply by adjusting the speed of both pumps. Since the maximum dosing capacity of the pumps, driven by stepper motors, was determined by the motor momentum and bubble breaking in the tee connector, higher velocities were obtained by using capillaries of smaller diameters. In this way it was possible to obtain linear velocities in the range 0.01–0.4 m/s. When the mass transfer coefficient was measured in capillaries of smaller diameters, the experiments were carried out also at low velocities in order to make a comparison between the determined mass transfer coefficients obtained with different capillaries within the same velocity range.

Calculation of experimentally determined mass transfer coefficients

Determination of the $k_L a$ coefficient. To determine the $k_L a$ coefficient at particular operating conditions, two runs were needed in order to eliminate the influence of inlet and outlet parts of the apparatus on measured data. The following assumptions were made during the calculation of $k_L a$ coefficients: (1) plug flow of the liquid phase, and (2) constant equilibrium methane concentration along the capillary. For the plug-flow model, the integral equation for the calculation of the $k_L a$ coefficient can be written as

$$k_L a = \frac{v}{L} \ln \frac{C^* - C_{in}}{C^* - C_{out}} \quad (1)$$

In all runs the inlet liquid was free of methane, hence, $C_{in} = 0$. During the experiments, effluent concentrations from the phase separator were measured; the outlet concentrations from the capillaries were calculated from data obtained in full and bare (without capillary) experimental set-ups. Since the volume, and thus the residence time of liquid in the tee connector, are small compared to those in capillaries and the phase separator, the mass of the methane transferred into water in the tee connector was neglected. Due to the same hydrodynamic conditions in the phase separator, the end effects in both experiment set-ups were assumed to be equal. Writing the former equation for both cases and expressing the outlet concentration from the capillaries with effluent concentrations measured in the full and the bare experimental set-ups, we derived the following correlation, which was used for the determination of experimentally measured $k_L a$ coefficients:

$$k_L a = \frac{v}{L} \ln \frac{C^* - C_{out}^{bare}}{C^* - C_{out}^{full}} \quad (2)$$

Determination of the $k_S a$ coefficient. Since the portion of the capillary length where the mass transfer takes place is determined by the length of impregnated tube, the $k_S a$ coefficient was determined by the

use of eq. (1). In most cases the inlet concentration of benzoic acid was zero, therefore, eq. (1) for the calculation of the $k_S a$ coefficient reads

$$k_S a = \frac{v}{L} \ln \frac{C^*}{C^* - C_{out}} \quad (3)$$

It should be noted that during $k_S a$ measurement capillary geometry was changing due to the dissolving of benzoic acid into the liquid passing through the capillary. To obtain more useful data from one experiment, the amount of liquid fed through the tube was weighed and appropriate corrections of the average tube ID, velocity and unit cell lengths were made by using mass flow data and measured concentrations. Although the actual channel became conical, cylindrical correction was used, and recalculations were made by using the average tube diameter. Without these corrections, the systematic error regarding the determination of velocity could be as high as 12%.

RESULTS AND DISCUSSION

The apparatus used in the present work allowed us to carry out experiments in such a way that one parameter (i.e. gas bubble length, liquid slug length, unit cell length, velocity or gas hold-up) was kept constant, while all other parameters could be varied. This enabled us to separately determine the partial influence of each particular parameter on the mass transfer, nitrite conversion and measured RTD dependencies. The experimentally obtained values of $k_L a$, $k_S a$ and the measured reaction conversion in capillaries operated under Taylor flow regime are shown in Figs 1–4, 7 and 8. This enabled us to find out which parameter has the greatest influence on the measured transport coefficients and obtained conversions. From Figs 1 and 3 one can see that the influence of velocity on the measured mass transport coefficients at different unit cell lengths can be expressed

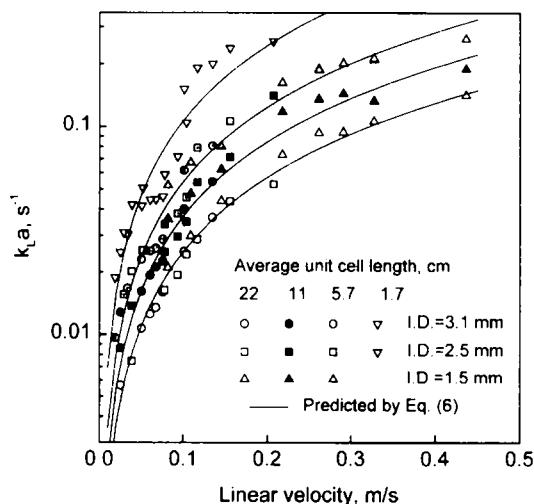


Fig. 1. Influence of velocity and unit cell length on measured $k_L a$ coefficients at fixed gas hold-up.

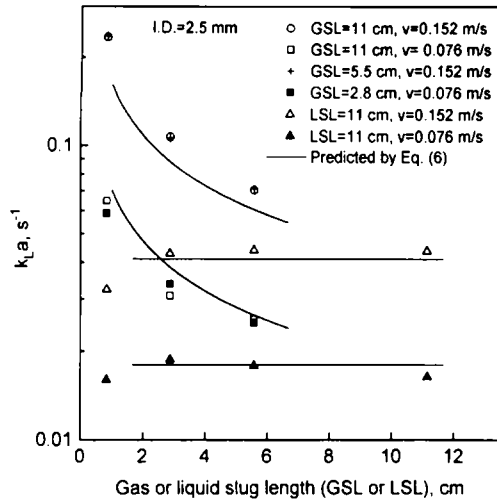


Fig. 2. Influence of liquid slug lengths or bubble lengths on measured $k_L a$ coefficients at fixed bubble length or constant liquid slug length.

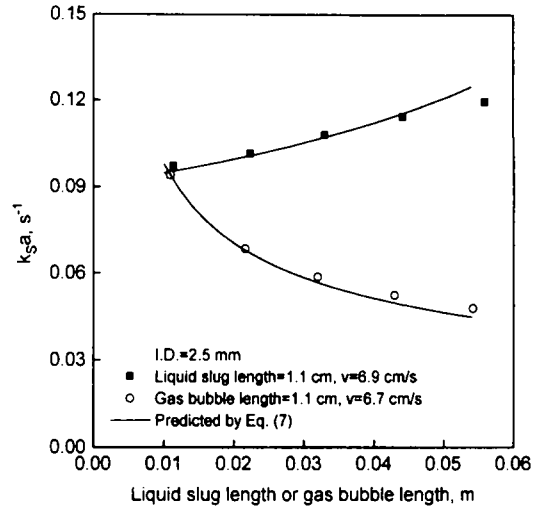


Fig. 4. Influence of liquid slug lengths or bubble lengths on measured $k_S a$ coefficients at fixed bubble length or fixed liquid slug length.

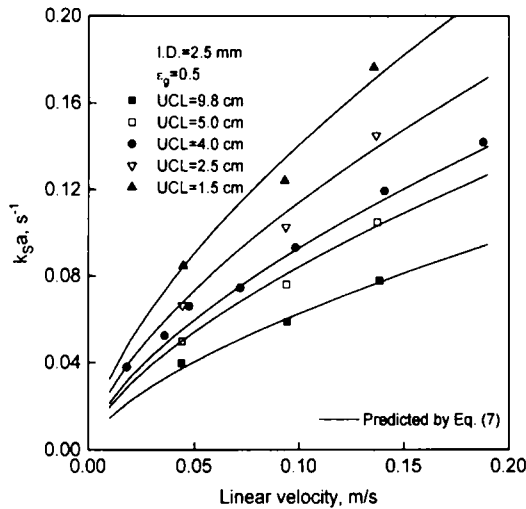


Fig. 3. Influence of velocity and unit cell length on measured $k_S a$ coefficients at fixed gas hold-up.

by the power function, as follows:

$$k_{L,S} a = p_1' v^{p_2} \quad (4)$$

If we compare the values of mass transfer coefficients measured at constant velocities but different unit cell lengths, we observe that the mass transfer coefficients $k_L a$ and $k_S a$ are inversely proportional to the length of the unit cell. This relation can be written as

$$k_{L,S} a = p_1'' / \text{UCL}^{p_3} \quad (5)$$

Figures 2 and 4 present the influence of the gas hold-up, i.e. the separate impact of gas bubble lengths at a fixed liquid slug length and the influence of liquid slug lengths at a fixed gas bubble length on mass transfer coefficients. It can be noticed that the length of liquid slugs influences the mass transport much more than the length of gas bubbles. While the former

dependency follows the previously determined influence of the unit cell length (measured at a constant gas hold-up), the influence of bubble length on the measured mass transport coefficients is almost negligible; therefore, a corrected form of eq. (5), which accounts also for gas hold-up, can be written for $k_L a$ as

$$k_L a = p_1 v^{p_2} / ((1 - \epsilon_G) \text{UCL})^{p_3} \quad (6)$$

and for $k_S a$ as

$$k_S a = p_1 v^{p_2} / ((1 - \epsilon_G) \text{UCL} - p_4 \text{UCL} \epsilon_G)^{p_3} \quad (7)$$

where the second term in the denominator of eq. (7) accounts for the decrease of liquid slug length and is proportional to the amount of liquid in the liquid film between the gas bubble and the wall. By means of non-linear regression (Duggleby, 1984), the values of parameters were calculated separately for $k_L a$ and $k_S a$ data. The values of parameters as well as the calculated deviations are summarised in Table 1. One can see that velocity influences the $k_L a$ coefficient much more than the $k_S a$ coefficient, while the dependency concerning the unit cell lengths, e.g. the lengths of liquid slugs, is almost equivalent in both cases.

In Fig. 5, experimentally measured $k_L a$ values are compared with the predicted $k_L a$ values using eq. (6) and semi-theoretical correlation (8):

$$k_L a = 4[\delta(d - \delta)U_{av}y_m + DShd_B]/[d^2 \text{UCL}] \quad (8)$$

which was proposed by Irandoost *et al.* (1992). In this correlation the first term accounts for mass transfer into liquid film between the gas bubble and the wall, while the second-term considers the mass transferred through spherical ends of liquid slugs. It should be noted that the parameters δ , U_{av} , y_m and Sherwood number are dependent on velocity, while the parameter y_m is dependent also on the length of gas slugs. The calculation procedure for prediction of the mixed-cup concentration (y_m) of solute in liquid film as well as the calculation of the average velocity (U_{av})

Table 1. Calculated values of parameters for equations describing mass transfer between gas and liquid [eq. (6)] and between liquid and solid [eq. (7)]

Equation (6)			Equation (7)		
Parameter	Value	Deviation	Parameter	Value	Deviation
p_1	0.111	± 0.006	p_1	0.069	± 0.0063
p_2	1.19	± 0.02	p_2	0.63	± 0.022
p_3	0.57	± 0.02	p_3	0.44	± 0.02
			p_4	0.105	± 0.015

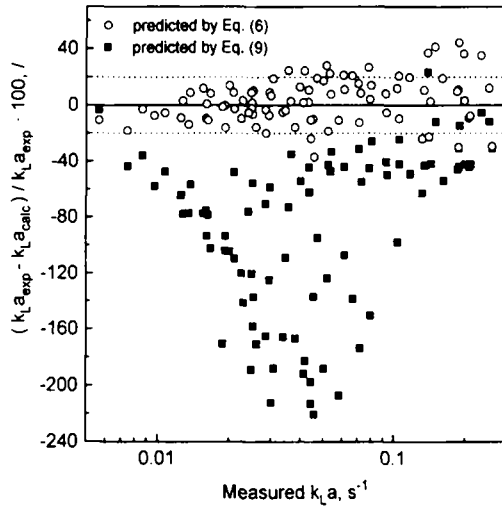


Fig. 5. Normalised residuals calculated by eqs (6) and (9) plotted against the experimentally measured $k_L a$ values.

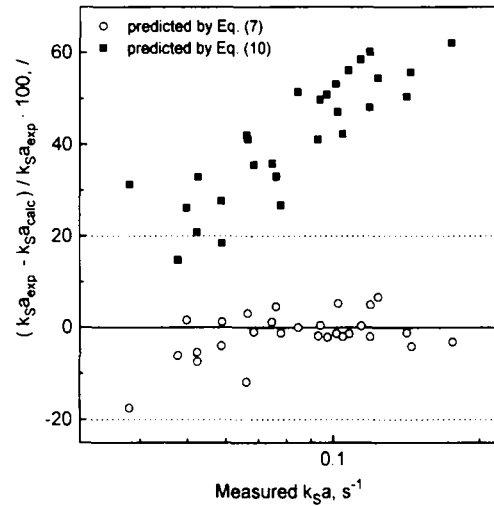


Fig. 6. Normalised residuals calculated by eqs (7) and (10) plotted against the experimentally measured $k_S a$ values.

of the liquid film are described in detail in the original paper. When the semi-theoretical equation was used for prediction of $k_L a$ coefficients, Irandoust *et al.* (1992) found out that good agreement with the measured data could be obtained if the experimentally determined $k_L a$ values were multiplied by a proportional factor α , thus,

$$k_L a = \alpha (k_L a)_{exp}. \quad (9)$$

By fitting procedure, they determined that α value equals to 0.686. In Fig. 5, the calculated values of $k_L a$ coefficients using corrected semi-theoretical correlation are compared with experimentally determined values. Evidently, the scattering is much higher than in the case of eq. (6). Almost all the predicted values are higher than the measured ones. This could be a consequence of the systematic error since the amount of gas transferred into the liquid in the inlet part of the apparatus they used was not considered. This caused that the values predicted by the proposed correlation are higher than those determined on this study. The large scattering of predicted $k_L a$ coefficients could be ascribed to an inadequately evaluated influence of studied parameters on the predicted $k_L a$ values.

Figure 6 shows similar comparison for $k_S a$ coefficients. On the ordinate-axis normalised differences

between experimentally determined values of $k_S a$ coefficient and those calculated by eq. (7) and correlation (10):

$$Sh = 3.51 \left(\frac{ReSc}{L/d} \right)^{0.44} \left(\frac{LSL}{d} \right)^{-0.09} \quad (10)$$

which was proposed by Hatzlantonou and Andersson (1988), are presented. To make comparison on the basis of $k_S a$ coefficients, the latter was expressed from the Sherwood number in former correlation. Both sides of the equation were multiplied by a specific area—which is for tubes equal to $4/d$ —in order to get functional dependency for $k_S a$ coefficient. From Fig. 6 we can see that the $k_S a$ coefficients calculated by eq. (7) show much lower scattering than the $k_S a$ coefficients calculated from correlation (10). The $k_S a$ values predicted by this correlation are smaller than those measured experimentally. This could be attributed to the downflow operation mode, which has smaller transport coefficients than the upflow operation mode used in our investigation. The same trend was observed by Kawakami *et al.* (1989). From the data presented in Fig. 6, one can further observe that the predicted values of $k_S a$ coefficients using correlation (10) exhibit a deviation trend, since the calculated differences increase with higher values of

k_{sa} coefficients. It is obvious also that this correlation does not ascribe for correct influence of the investigated parameters on the mass transfer in the segmented flow through capillaries. It should be stressed that the correlation (10) was derived on the basis of 12 experimental measurements, while the semi-theoretical correlation for prediction of $k_L a$ coefficients was derived from 30 experimental observations. Although these correlations should be general, i.e. useful for other components and reaction conditions, it is obvious from the confrontations shown in Figs 5 and 6 that they did not accurately predict the influence of investigated parameters on the measured mass transport coefficients. Therefore, the primary interest of this investigation was to find out which parameters are the most important and how they influence the mass transport coefficients. For derivation of generalised correlations, additional experiments with different components and at different operating conditions should be made.

In the following text, we try to verify the reported observations about mass transport in a capillary by comparing experimentally observed trends with the predicted ones using a hydrodynamic model for the description of axial dispersion in the Taylor flow regime. The proposed model was solved for two hypothetical conditions:

- complete saturation of the liquid film surrounding the gas bubble and;
- complete conversion of the reactant in the same film.

Figures 7 and 8 illustrate the experimentally measured conversions of nitrite ions during the heterogeneously catalysed liquid-phase hydrogenation carried out in a single-channel capillary reactor operated under the Taylor flow regime. It is evident that the relative influence of unit cell lengths is smaller if compared to the results presented for mass transfer measurements. This might be attributed to high mass transport and relatively slow reaction, which both ensure that the surface concentration was close to the one in the bulk phase of the liquid slug. When the reaction was carried out at different gas hold-up which was obtained by changing the lengths of gas bubbles at a fixed liquid slug length or by changing the liquid slug lengths at a constant gas bubble length, we can qualitatively distinguish between the extent of reaction in the liquid slug and in the liquid film surrounding a gas bubble. The trend of the measured conversion, obtained when the liquid slug length was increased, followed the previously determined dependencies for $k_L a$ and k_{sa} coefficients (Figs 2 and 4). Based on the results obtained during the mass transfer and chemical reaction studies at fixed liquid slug lengths one can assume that either the mass transfer as well as the reaction reach equilibrium in the liquid film, or that the extent of mass transport and the amount of reactant consumed in the liquid film is negligible compared to the one in the liquid slug; otherwise, the

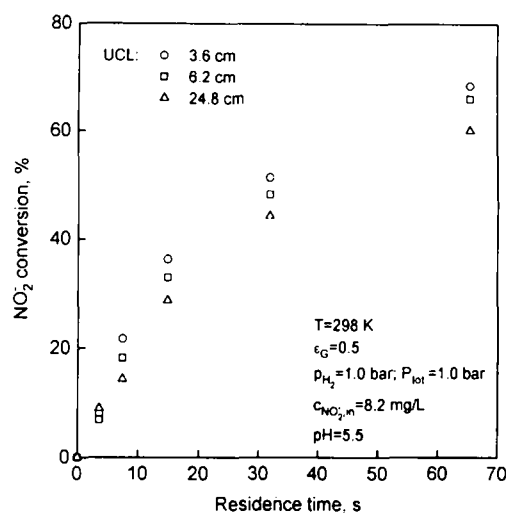


Fig. 7. Measured conversions of nitrite ions during the course of catalytic hydrogenation at different unit cell lengths.

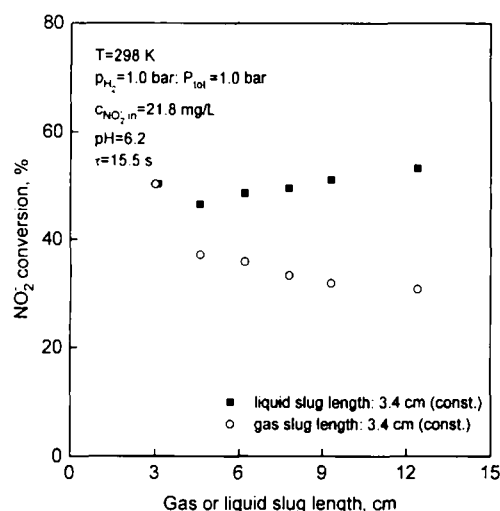


Fig. 8. Influence of liquid slug lengths or bubble lengths on measured conversion of nitrite ions at fixed bubble length or fixed liquid slug length.

measured conversion should increase with the increased gas bubble length more than it has been measured. To provide a solid ground for this discrimination, RTD measurements were carried out and the results will be discussed below also in the view of previously stated assumptions.

In capillaries operating under the Taylor flow it is difficult to obtain a sharp step input of tracer due to the dead volume between the tee connector and the solenoid valve used for switching between two feeding solutions of different tracer concentrations. Theoretically, it would be better to introduce the pulse input into one liquid slug, but this would be very difficult to perform experimentally without influencing the flow pattern. Therefore, we decided to study the axial dispersion by using the step input of tracer. Since the tracer concentrations were measured at two different

axial locations of the glass tube, the system can be viewed as an open vessel (Levenspiel, 1972). Due to the segmented flow through the capillary, the measured signal at a specific axial location is discontinuous. Creation of the F-curve and later differentiation in order to obtain the RTD curve would be uncertain due to the small numbers of liquid slugs which passed the detector before the inlet concentration was detected, especially at the measured position beside the inlet tee connector.

While developing a mathematical model for the prediction of axial dispersion in the capillaries operated under the Taylor flow, the results of a mathematical analysis which predicts the flow-patterns formed in the liquid slug and the gas bubble, were analysed qualitatively. By computer simulation, Irandoust *et al.* (1992) showed that the mixing of the liquid film into the succeeding liquid slug is incomplete, since the predicted results—when complete mixing is assumed overpredict the experimentally measured values.

On the basis of the simulated flow patterns in the liquid slug we assumed that the liquid slug can be described as a CSTR reactor with the inflow described by the following equation:

$$\phi_V^n = \pi(d^2 - (d - 2\delta)^2)v/4. \quad (11)$$

The volumetric outflow is equal to the inflow since a steady-state operation was assumed. However, such analysis would lead to overestimated results as it was shown by Irandoust *et al.* (1992). Therefore, we tested the CSTR by-pass model (Fogler, 1986) which can be described for the *i*th liquid slug as

$$\frac{dC_i}{dt} = (1 - \beta)\phi_v(C_{in} - C_i)/V \quad (12)$$

where the inlet concentration into the succeeding liquid slug was calculated as

$$C_{in}^{i+1} = \beta C_{in}^i + (1 - \beta)C_i. \quad (13)$$

The factor $(1 - \beta)$ represents the fraction of the inlet film which is mixed with the liquid slug, while fraction β of the inlet film bypasses the liquid slug. Since the thickness of the liquid film is a function of fluid properties and velocity, the thickness of the liquid film was calculated according to the correlation proposed by Irandoust and Andersson (1988):

$$\delta = 0.18d\{1 - \exp[-3.1(\mu v/\sigma)^{0.54}]\}. \quad (14)$$

For each liquid slug, the concentration at axial location 2 ($L = 102$ cm) was calculated on the basis of the experimentally measured values at axial location 1 ($L = 15.5$ cm). The number of slugs used for the calculation was determined on the basis of measured concentration at the location 2. Only those slugs were considered in which the measured concentrations were below 99.5% of the used tracer concentration. The value of parameter β was calculated by means of the non-linear regression method. Marquardt optimisation technique (Duggleby, 1984) was coupled

Table 2. Fitted values of model parameter β

Average UCL $\times 10^2$ (m)	Velocity $\times 10^2$ (m/s)	β^*
3.6	5.4	0.722
5.5	5.4	0.733
7.3	5.4	0.629
9.1	5.4	0.62
18.2	5.4	0.729
3.6	2.8	0.584
3.6	1.4	0.545
3.6	0.7	0.52

Linearised correlation for β : $\beta = 3.553v + 0.492$.

with the fifth-order Cash–Karp Runge–Kutta integration algorithm (Press *et al.*, 1992). The latter was used while calculating the sum of residuals, which was minimized in order to calculate the values of tracer concentration in liquid slugs at location 2. The sum of weighted residuals was calculated as

$$S_R = \sum_{i=1}^n (C_{out,i}^{exp} - C_{out,i}^{calc})^2 W_i \quad (15)$$

where the weighting factor, W_i , was set proportional to $(1/C_{out,i}^{exp})^2$ in order to distribute the calculated deviation proportionally among all points regardless of their absolute value. During minimization, the system of equations was formed on the basis of basic model eqs (12) and (13) for all points used. The resulting set of coupled equations was integrated using the previously mentioned method for the time period which was calculated from the distance between the measured locations and the average velocity. The inlet concentration entering the first liquid slug was always zero, while for all other liquid slugs the inlet concentrations were calculated according to relation (13). The calculated values of parameter β are summarised in Table 2 for different operating conditions. It can be seen that parameter β is almost independent of the unit cell length, but depends rather on velocity. However, it should be noted that velocity influences also the thickness of the liquid film according to eq. (14). For the range of operating conditions used during RTD measurements, the influence of velocity on parameter β can be linearised and calculated by the following equation:

$$\beta = 0.492 + 3.553v. \quad (16)$$

The comparison between measured concentrations in liquid slugs at location 2 and those calculated by the proposed model is shown in Figs 9 and 10. It is obvious that good agreement was obtained and that the model predicts hydrodynamic behaviour of the Taylor flow at the examined experimental conditions quite well.

To evaluate the influence of the thin liquid film between the gas bubble and the wall of the capillary on the mass-transfer between gas and liquid and the extent of nitrite transformation, the proposed model

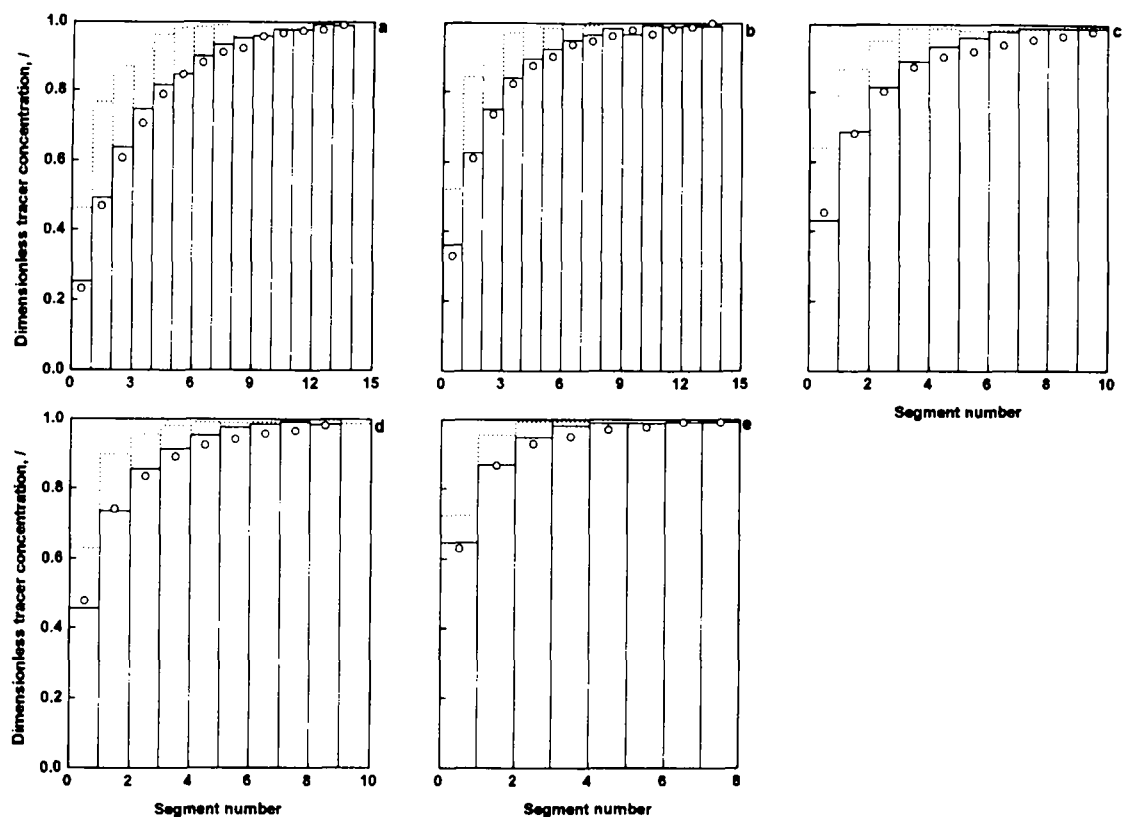


Fig. 9. Comparison between measured and predicted tracer concentrations in liquid slugs at location $L = 102$ cm for different unit cell lengths used: (a) 3.6; (b) 5.5; (c) 7.3; (d) 9.1; (e) 18.2 cm. Velocity: 5.4 cm/s. Dotted lines represent measured concentrations at location $L = 15.5$ cm; solid lines correspond to those measured at location 102 cm.

Table 3. Comparison between measured and predicted concentrations of methane in water during $k_L a$ measurements (ID = 2.56 mm, $L = 112$ cm)

(Average* length of gas bubble and liquid slug) $\times 10^2$ (m)		Average velocity 7.6×10^{-2} (m/s) Concentrations of methane at the outlet of capillary (mg/l)		Average velocity 3.7×10^{-2} (m/s)	
Gas	Liquid	Measured	Predicted	Measured	Predicted
11	11	4.8	2.9	4.4	3.2
5.5	5.5	6.9	5.5	7.4	5.5
2.8	2.8	9.0	9.5	9.8	9.9
0.9	0.9	12.9	19.1	15.8	19.5
11	5.5	7.0	5.8		
11	2.8	8.2	10.8		
5.5	11	5.1	2.9		
2.8	11	5.4	2.8		

* Calculated on the basis of feed amount of liquid or gas to form one slug or bubble, i.e. feed volume divided by cross-section area of the capillary. Correction due to liquid film is not considered.

was solved for two extreme hypothetical cases already mentioned. The results are summarised in Tables 3 and 4. It is clear from the comparison between the measured and predicted methane concentrations in the outcoming liquid from the capillary, that, when the length of liquid slugs was decreased, predicted

methane concentrations increase faster than the measured ones. When the liquid slug length was kept constant, the trend between the predicted and measured concentrations was the same, i.e. the measured concentrations as well as those predicted were almost independent of the gas bubble length. When the

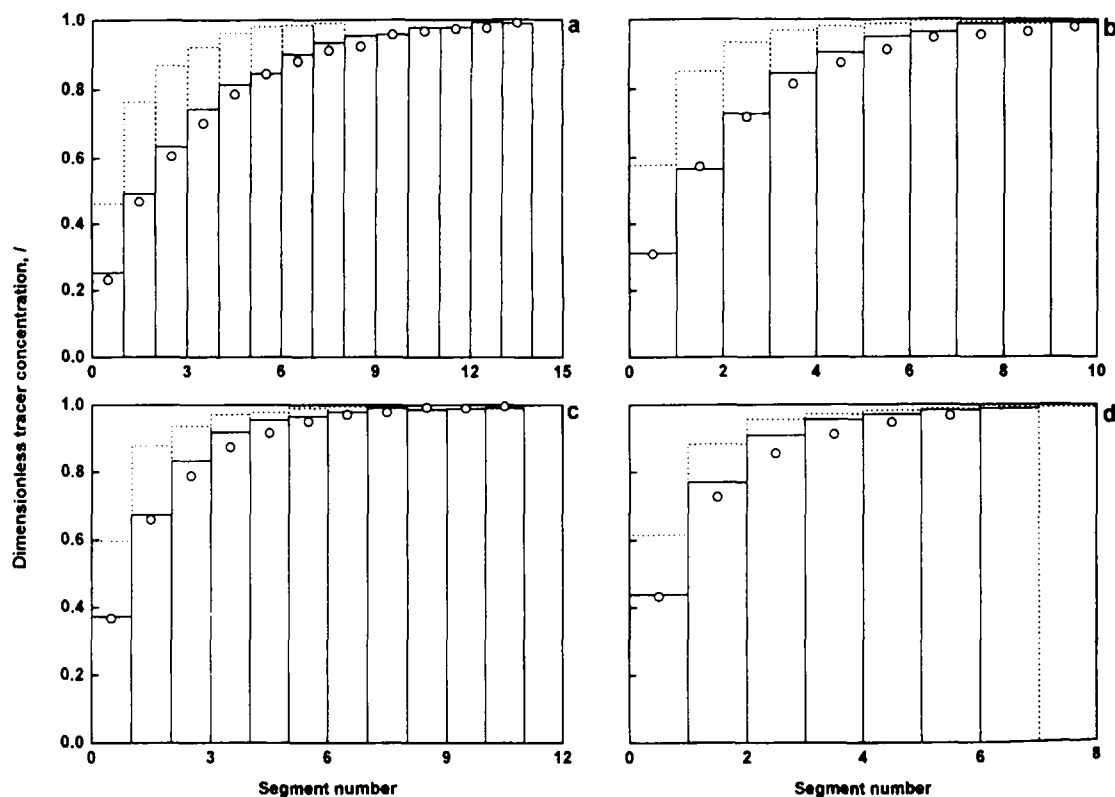


Fig. 10. Influence of velocity on measured and predicted tracer concentrations at axial location 102 cm: (a) 5.4; (b) 2.8; (c) 1.4; (d) 0.7 cm/s. UCL: 3.6 cm. For legend see Fig. 9.

Table 4. Comparison between measured and predicted nitrite conversion during the catalytic hydrogenation of nitrite ions in capillary coated with *Pd* (ID = 1.85 mm, *L* = 112 cm)

(Average* length of gas bubble and liquid slug)×10 ² (m)		Nitrite conversion			
		Average velocity = 7.2 × 10 ⁻² (m/s)		Average velocity = 3.6 × 10 ⁻² (m/s)	
Gas	Liquid	Measured	Predicted	Measured	Predicted
C _{NO₂,in} = 21.8 mg/l, pH = 6.2					
3.1	3.1	50.2	38.8		
6.2	3.1	48.5	40.5		
9.3	3.1	51.4	43		
12.4	3.1	53.2	44.3		
3.1	6.2	35.8	20.3		
3.1	9.3	31.9	14.7		
3.1	12.4	30.7	11.2		
C _{NO₂,in} = 8.2 mg/l, pH = 5.5					
1.8	1.8	36.3	56.0	51.3	57.3
3.1	3.1	32.9	38.9	48.2	39.9
12.4	12.4	28.6	11.6	44.1	12.1

* Calculated on the basis of feed amount of liquid or gas to form one slug or bubble, i.e. feed volume divided by cross-section area of the capillary. Correction due to liquid film is not considered.

results measured at two different velocities but the same UCL are compared with the predicted ones, it is evident that the predicted trend does not follow the measured one; the predicted data at two different

velocities are almost equal for all cases, while the measured values show considerable differences.

The same conclusions could be drawn also from the results presented in Table 4, where the effect of

different lengths of liquid slugs and gas bubbles on measured conversion is shown. The measured and calculated nitrite conversions at the same liquid slug lengths are almost independent of the length of gas bubbles. When the UCL was decreased, the predicted values showed much higher dependency on the UCL than it was observed experimentally. The predicted conversions at two different velocities are almost equal, while experimentally considerable differences were determined. It arises from the presented simulations applying the two unrealistic assumptions mentioned before that the predictions made by the proposed model do not follow the experimentally observed trends. Based on the above discussion it can be concluded that for mass transfer, as well as for liquid-phase nitrite reduction experiments, the lengths of liquid slugs are of the highest importance. The major part of the mass which is transferred between the gas and the liquid phase goes through the spherical-ended surface of liquid slugs, while the major part of the reaction is performed on the surface of the catalytic active capillary which is covered by the liquid slug.

CONCLUSIONS

A CSTR by-pass model has been proposed for the description of the Taylor flow through capillaries. It is obvious from the comparison between experimental and predicted data that the most important parameters for the determination of mass transfer under the Taylor flow regime are the cell velocity and the length of the liquid slugs. The major part of mass transfer between the gas and liquid phases and the catalyst surface is performed through surfaces exposed to liquid slugs and not through gas bubbles as it was assumed earlier.

Acknowledgement

The authors gratefully acknowledge the financial support from the Slovenian Ministry of Science and Technology under grant No. 7031-0104-95.

NOTATION

C	concentration, mg/l
C^*	equilibrium concentration, mg/l
d	internal diameter of capillary, m
D	diffusion coefficient, m^2/s
k_{La}	gas-liquid mass transfer coefficient, s^{-1}
k_{sa}	liquid-solid mass transfer coefficient, s^{-1}
L	length of capillary, m
n	number of liquid slugs, dimensionless
p_1'	parameter in eq. (4), $\text{s}^{p_2-1} \text{m}^{-p_2}$
p_1''	parameter in eq. (5), $\text{m}^{p_3} \text{s}^{-1}$
p_1	parameter in eqs (6) and (7), $\text{s}^{p_2-1} \text{m}^{p_3-p_2}$
p_2	parameter in eqs (6) and (7), dimensionless
p_3	parameter in eqs (6) and (7), dimensionless
p_4	parameter in eq. (7), dimensionless
Re	Reynolds number, dimensionless
Sc	Schmidt number, dimensionless
Sh	Sherwood number, dimensionless
S_R	weighted sum of residuals, dimensionless

U_{av}	average velocity in the liquid film, m/s
UCL	unit cell length (the length of one gas bubble plus one liquid slug), m
v	average cell velocity, m/s
V	volume of a liquid slug, m^3
W	weighted factor, $(\text{l}\cdot\text{m}^3)^2$

Greek letters

α	proportional factor in eq. (9), dimensionless
β	parameter in eq. (12), dimensionless
δ	liquid film thickness, m
ϵ_G	gas hold-up, dimensionless
μ	liquid viscosity, $\text{kg}/\text{m}\cdot\text{s}$
σ	surface tension, N/m
τ	residence time, s
ϕ	volumetric flow, m^3/s

Subscripts/superscripts

calc	calculated
exp	experimental
i	i th slug
in	inlet
out	outlet

REFERENCES

- Bretherton, F. P. (1961) The motion of long bubbles in tubes. *J. Fluid Mech.* **10**, 166-188.
- Crynes, L. L., Cerro, R. I. and Abraham, M. A. (1995) Monolith froth reactor: development of a novel three-phase catalytic system. *A.I.Ch.E. J.* **41**, 337-345.
- Cybulski, A., Edvinsson, R. K., Irandoust, S. and Andersson, B. (1993) Liquid-phase methanol synthesis: modelling of a monolith reactor. *Chem. Engng Sci.* **48**, 3463-3478.
- Duggleby, R. G. (1984) Regression analysis of nonlinear Arrhenius plots: an empirical model and a computer program. *Comput. Biol. Med.* **14**, 447-455.
- Edvinsson, R. K. and Irandoust, S. (1996) Finite-element analysis of Taylor flow. *A.I.Ch.E. J.* **42**, 1815-1823.
- Fairbrother, F. and Stubbs, A. (1935) Studies in electro-endosmosis Part VI. The bubble-tube methods of measurement. *J. Chem. Soc. D-Chem. Commun.* **1**, 527-529.
- Fogler, H. S. (1986) *Elements of Chemical Reaction Engineering*, p. 692. Prentice-Hall, Englewood Cliffs, NJ, U.S.A.
- Hatzlantonidou, V. and Andersson, B. (1982) Solid-liquid mass transfer in segmented gas-liquid flow through a capillary. *Ind. Engng Chem. Fundam.* **21**, 451-456.
- Irlandoust, S. and Andersson, B. (1988) Mass transfer and liquid-phase reactions in a segmented two-phase flow monolith catalytic reactor. *Chem. Engng Sci.* **43**, 1983-1988.
- Irlandoust, S., Andersson, B., Bengtsson, E. and Siverström, M. (1989) Scaling up of a monolithic catalyst reactor with two-phase flow. *Ind. Engng Chem. Res.* **28**, 1489-1495.
- Irlandoust, S., Ertle, S. and Andersson, B. (1992) Gas-liquid mass transfer in Taylor flow through a capillary. *Can. J. Chem. Engng* **70**, 115-119.
- Kawakami, K., Kawasaki, K., Shiraishi, F. and Kusunoki, K. (1989) Performance of a honeycomb

- monolith bioreactor in a gas-liquid-solid three-phase system. *Ind. Engng Chem. Res.* **28**, 394-400.
- Levenspiel, O. (1972) *Chemical Reaction Engineering*, 2nd Edn. Wiley, New York, U.S.A.
- Marchessault, R. N. and Mason, S. G. (1960) Flow of entrapped bubbles through a capillary. *Ind. Engng Chem.* **52**, 79-84.
- Patrick, R. H., Klindera, T., Crynes, L. L., Cerro, R. L. and Abraham, M. A. (1995) Residence time distribution in three-phase monolith reactor. *A.I.Ch.E. J.* **41**, 649-657.
- Pedersen, H. and Horváth, C. (1981) Axial dispersion in a segmented gas-liquid flow. *Ind. Engng Chem. Fundam.* **20**, 181-186.
- Press, W. H., Teukolovsky, S. A., Vetterling, W. T. and Flannery, B. P. (1992) *Numerical Recipes in Fortran*, 2nd Edn. Cambridge University Press, Cambridge.
- Shen, E. I. and Udell, K. S. (1985) A finite element study of low Reynolds number two-phase flow in cylindrical tubes. *J. Appl. Mech.-Trans. ASME* **52**, 253-256.
- Taylor, G. I. (1960) Deposition of viscous fluid on the wall of a tube. *J. Fluid Mech.* **10**, 161-165.
- Wärnå, J., Turunen, I., Salmi, T. and Maunula, T. (1994) Kinetics of nitrate reduction in monolith reactor. *Chem. Engng Sci.* **49**, 5763-5773.